EUROPEAN ORGANIZATION FOR NUCLEAR RESEARCH

CERN-PH-EP-2012-288
29 October 2012

Measurement of the branching ratio of the decay $\Xi^0 \rightarrow \Sigma^+\mu^-\overline{\nu}_\mu$

Abstract

From 56 days of data taking in 2002 with a neutral kaon beam, the NA48/1 experiment observed 97 $\Xi^0 \rightarrow \Sigma^+\mu^-\overline{\nu}_\mu$ candidates with a background contamination of 30.8 ± 4.2 events. From this sample, the BR($\Xi^0 \rightarrow \Sigma^+\mu^-\overline{\nu}_\mu$) is measured to be $(2.17 \pm 0.32_{\mathrm{stat}} \pm 0.17_{\mathrm{syst}}) \times 10^{-6}$.

J.R. Batley, G.E. Kalmus[1], C. Lazzeroni, D.J. Munday, M. Patel, M.W. Slater, S.A. Wotton
Cavendish Laboratory, University of Cambridge, Cambridge, CB3 0HE, UK[2]

R. Arcidiacono, G. Bocquet, A. Ceccucci, D. Cundy[3], N. Doble[4], V. Falaleev, L. Gatignon,
A. Gonidec, P. Grafström, W. Kubischta, F. Marchetto[5], I. Mikulec[6], A. Norton, B. Panzer-Steindel,
P. Rubin[7], H. Wahl[8]
CERN, CH-1211 Genève 23, Switzerland

E. Goudzovski, P. Hristov[9], V. Kekelidze, V. Kozhuharov, L. Litov, D. Madigozhin, N. Molokanova,
Yu. Potrebenikov, S. Stoynev, A. Zinchenko
Joint Institute for Nuclear Research, Dubna, Russian Federation

E. Monnier[10], E.C. Swallow[11], R. Winston[12]
The Enrico Fermi Institute, The University of Chicago, Chicago, Illinois, 60126, U.S.A.

R. Sacco[13], A. Walker
Department of Physics and Astronomy, University of Edinburgh, JCMB King's Buildings, Mayfield Road, Edinburgh, EH9 3JZ, U.K.

W. Baldini, P. Dalpiaz, P.L. Frabetti, A. Gianoli, M. Martini, F. Petrucci, M. Scarpa, M. Savrié
Dipartimento di Fisica dell'Università e Sezione dell'INFN di Ferrara, I-44100 Ferrara, Italy

A. Bizzeti[14], M. Calvetti, G. Collazuol[15], E. Iacopini, M. Lenti, G. Ruggiero[9], M. Veltri[16]
Dipartimento di Fisica dell'Università e Sezione dell'INFN di Firenze, I-50125 Firenze, Italy

M. Behler, K. Eppard, M. Eppard, A. Hirstius, K. Kleinknecht, U. Koch, L. Masetti, P. Marouelli,
U. Moosbrugger, C. Morales Morales[17], A. Peters[9], R. Wanke, A. Winhart
Institut für Physik, Universität Mainz, D-55099 Mainz, Germany[18]

A. Dabrowski, T. Fonseca Martin[9], M. Velasco
Department of Physics and Astronomy, Northwestern University, Evanston Illinois 60208-3112, U.S.A.

G. Anzivino, P. Cenci, E. Imbergamo, G. Lamanna[19], P. Lubrano, A. Michetti, A. Nappi, M. Pepe,
M.C. Petrucci, M. Piccini[20], M. Valdata
Dipartimento di Fisica dell'Università e Sezione dell'INFN di Perugia, I-06100 Perugia, Italy

C. Cerri, F. Costantini, R. Fantechi, L. Fiorini[21], S. Giudici, I. Mannelli, G. Pierazzini, M. Sozzi
Dipartimento di Fisica, Scuola Normale Superiore e Sezione dell'INFN di Pisa, I-56100 Pisa, Italy

C. Cheshkov, J.B. Cheze, M. De Beer, P. Debu, G. Gouge, G. Marel, E. Mazzucato, B. Peyaud,
B. Vallage
DSM/DAPNIA - CEA Saclay, F-91191 Gif-sur-Yvette, France

M. Holder, A. Maier, M. Ziolkowski
Fachbereich Physik, Universität Siegen, D-57068 Siegen, Germany[22]

S. Bifani, C. Biino, N. Cartiglia, M. Clemencic, S. Goy Lopez, E. Menichetti, N. Pastrone
Dipartimento di Fisica Sperimentale dell'Università e Sezione dell'INFN di Torino, I-10125 Torino, Italy

W. Wislicki,
Soltan Institute for Nuclear Studies, Laboratory for High Energy Physics, PL-00-681 Warsaw, Poland[23]

H. Dibon, M. Jeitler, M. Markytan, G. Neuhofer, L. Widhalm
Österreichische Akademie der Wissenschaften, Institut für Hochenergiephysik, A-10560 Wien, Austria[24)]

NA48/1 collaboration

---

[1] Present address: Rutherford Appleton Laboratory, Chilton, Didcot, OX11 0QX, UK

[2] Funded by the U.K. Particle Physics and Astronomy Research Council

[3] Present address: Instituto di Cosmogeofisica del CNR di Torino, I-10133 Torino, Italy

[4] Also at Dipartimento di Fisica dell'Università e Sezione dell'INFN di Pisa, I-56100 Pisa, Italy

[5] On leave from Sezione dell'INFN di Torino, I-10125 Torino, Italy

[6] On leave from Österreichische Akademie der Wissenschaften, Institut für Hochenergiephysik, A-1050 Wien, Austria

[7] On leave from University of Richmond, Richmond, VA, 23173, USA; supported in part by the US NSF under award #0140230. Present address: Department of Physics and Astronomy George Mason University, Fairfax, VA 22030A, USA

[8] Also at Dipartimento di Fisica dell'Università e Sezione dell'INFN di Ferrara, I-44100 Ferrara, Italy

[9] Present address: CERN, CH-1211 Genève 23, Switzerland

[10] Present address: Centre de Physique des Particules de Marseille, IN2P3-CNRS, Université de la Méditerranée, Marseille, France

[11] Present address: Department of Physics, Elmhurst College, Elmhurst, IL, 60126, USA

[12] Also at University of California, Merced, USA

[13] Present address: Department of Physics Queen Mary, University of London, Mile End Road, London E1 4NS, United Kingdom

[14] Dipartimento di Fisica dell'Università di Modena e Reggio Emilia, via G. Campi 213/A I-41100, Modena, Italy

[15] Present address: Scuola Normale Superiore e Sezione dell'INFN di Pisa, I-56100 Pisa, Italy

[16] Istituto di Fisica, Università di Urbino, I-61029 Urbino, Italy

[17] Present address: Institut für Kernphysik, Universität Mainz, D-55099 Mainz, Germany

[18] Funded by the German Federal Minister for Research and Technology (BMBF) under contract 7MZ18P(4)-TP2

[19] Present address: Dipartimento di Fisica e Sezione dell'INFN di Pisa, I-56100 Pisa, Italy

[20] contact: Mauro.Piccini@pg.infn.it

[21] Present address: Cavendish Laboratory, University of Cambridge, Cambridge, CB3 0HE, U.K.

[22] Funded by the German Federal Minister for Research and Technology (BMBF) under contract 056SI74

[23] Supported by the Committee for Scientific Research grants 5P03B10120, SPUB-M/CERN/P03/DZ210/2000 and SPB/CERN/P03/DZ146/2002

[24] Funded by the Austrian Ministry for Traffic and Research under the contract GZ 616.360/2-IV GZ 616.363/2-VIII, and by the Fonds für Wissenschaft und Forschung FWF Nr. P08929-PHY

1 Introduction

The study of hadron beta decays gives important information on the interplay between the weak interaction and hadron structure determined by the strong interaction. In this context the Ξ^0 semileptonic decay represents an extraordinary opportunity to test both the SU(3) symmetry, via its strong analogy with the well known neutron beta decay, and the quark mixing model [1] via the $V_{\rm us}$ extraction. In particular, a clear evidence for the decay $\Xi^0 \to \Sigma^+ \mu^- \overline{\nu}_\mu$ and a measurement of its branching ratio will add one more constraint to test the theoretical frameworks [2, 3, 4, 5, 6] built to explain and to predict the behaviors of the hadron semileptonic decays.

In the present article the branching ratio of the semileptonic decay $\Xi^0 \to \Sigma^+ \mu^- \overline{\nu}_\mu$ is measured by normalizing to the analogue decay with an electron in the final state, already studied by the NA48/1 collaboration [7]. The similar topologies of the final states of the two semileptonic decays allowed the same trigger conditions to be used for both data samples. The selection criteria are also similar between the two channels and only differ for the identification of the charged lepton and for cuts related to background rejection. This decay had already been observed by the KTeV collaboration [8], with a sample of 9 events and a branching ratio measurement of $(4.7^{+2.2}_{-1.6}) \times 10^{-6}$.

2 Beam

The experiment was performed in 2002 at the CERN SPS accelerator and used a 400 GeV proton beam impinging on a Be target to produce a neutral beam. The spill length was 4.8 s out of a 16.2 s cycle time. The proton intensity was fairly constant during the spill with a mean of 5×10^{10} particles per pulse.

For this measurement, only the K_S target station of the NA48 double K_S/K_L beam line [9] was used to produce the neutral beam. In this configuration, the K_L beam was blocked and an additional sweeping magnet was installed to deflect charged particles away from the defining section of the K_S collimators. To reduce the number of photons in the neutral beam originating primarily from π^0 decays, a 24 mm thick platinum absorber was placed in the beam between the target and the collimator. A pair of coaxial collimators, having a total thickness of 5.1 m, the axis of which formed an angle of 4.2 mrad to the proton beam direction, selected a beam of neutral long-lived particles (K_S, K_L, Λ^0, Ξ^0, n and γ). The target position and the production angle were chosen in such a way that the beam axis was hitting the center of the electromagnetic calorimeter.

In order to minimize the interaction of the neutral beam with air, the collimator was immediately followed by a 90 m long evacuated tank terminated by a 0.3% X_0 thick Kevlar window. The NA48 detector was located downstream of this region.

On average, about 1.4×10^4 Ξ^0 per spill, with an energy between 70 and 220 GeV, decayed in the fiducial decay volume.

3 Detector

The detector was designed for the measurement of $Re(\varepsilon'/\varepsilon)$, and a detailed description of the experimental layout is available at [9]. In the following sections a short description of the main detectors is reported.

3.1 Tracking

The detector included a spectrometer housed in a helium gas volume with two drift chambers before and two after a dipole magnet with an horizontal transverse momentum kick of 265 MeV/c. Each chamber had four views (x, y, u, v), each of which had two sense wire planes. The resulting space points were typically reconstructed with a resolution of $\sim$ 150 μm in each projection. The spectrometer momentum resolution is parameterized as:

$$\sigma_p/p = 0.48\% \oplus 0.015\% \times p$$

where p is in GeV/c. This gave a resolution of 3 MeV/c^2 when reconstructing the kaon mass in $K^0 \to \pi^+\pi^-$ decays. The track time resolution was $\sim$ 1.4 ns.

3.2 Electromagnetic Calorimetry

The detection and measurement of the electromagnetic showers were achieved with a liquid krypton calorimeter (LKr), 27 radiation lengths deep, with a $\sim$2 cm $\times$ 2 cm cell cross-section.

The energy resolution, expressing E in GeV, is parameterized as [9]:

$$\sigma(E)/E = 3.2\%/\sqrt{E} \oplus 9\%/E \oplus 0.42\%$$

The transverse position resolution for a single photon of energy larger than 20 GeV was better than 1.3 mm, and the corresponding mass resolution for the reconstructed π^0 mass ($\gamma\gamma$ decay) was $\sim$1 MeV/c^2. The time resolution of the calorimeter for a single shower was better than $\sim$ 300 ps.

3.3 Scintillator Detectors and Muon Detector

A scintillator hodoscope (CHOD) was located between the spectrometer and the calorimeter. It consisted of two planes, segmented in horizontal and vertical strips and arranged in four quadrants. Further downstream there was an iron-scintillator sandwich hadron calorimeter (HAC), followed by muon counters consisting of three planes of scintillator, each shielded by an 80 cm thick iron wall. The first two planes $M1X$ and $M1Y$ were the main muon counters and had 25 cm wide horizontal and vertical scintillator strips respectively, with a length of 2.7 m. The third plane, $M2X$, had horizontal strips 44.6 cm wide, and was mainly used to measure the efficiency of the $M1X$ and $M1Y$ counters. The central strip in each plane was divided into two sections separated by a gap of 21 cm, in order to accommodate the beam pipe. The fiducial volume of the experiment was principally determined by the LKr calorimeter acceptance, together with seven rings of scintillation counters (AKL) used to veto activity outside this region.

4 Trigger

The trigger system used for the on-line selection of Ξ^0 semileptonic decays mainly consisted of two levels of logic. Level 1 (L1) was based on logic combinations of fast signals coming from various subdetectors. It required hits in the CHOD and in the first drift chamber compatible with at least one and two tracks respectively, no hit in the AKL veto system and a minimum energy deposition in the calorimeters. This last requirement was 15 GeV for the energy reconstructed in the LKr calorimeter or 30 GeV for the summed energy in the electromagnetic and hadronic calorimeters. The output rate of the L1 stage was about 50 kHz. The average L1 efficiency, measured with $\Xi^0 \to \Lambda\pi^0$ events of energy greater than 70 GeV, was found to be $98.65 \pm 0.03\%$.

Level 2 (L2) consisted of a set of 300 MHz processors that reconstructed tracks and vertices from hits in the drift chambers and computed relevant physical quantities. The L2 trigger required at least two tracks with a closest distance of approach of less than 8 cm in space and a transverse separation greater than 5 cm in the first drift chamber. Since the signature of the Ξ^0 β-decay involves the detection of an energetic proton from the subsequent $\Sigma^+ \to p\pi^0$ decay, the ratio between the higher and the lower of the two track momenta was required to be larger than 3.5. Rejection of the overwhelming $\Lambda \to p\pi^-$ and

$K_S \to \pi^+\pi^-$ decays was achieved by applying stringent invariant mass cuts against these decays. The output L2 trigger rate was about 2.5 kHz. The efficiency of the L2 trigger stage with respect to Level 1, averaged over the 2002 run, was measured to be $(83.7 \pm 2.2)\%$ for Ξ^0 β-decays, mainly limited by wire inefficiencies in the drift chambers.

5 Offline selection

The identification of the $\Xi^0 \to \Sigma^+\mu^-\overline{\nu}_\mu$ channel was performed using the subsequent decay $\Sigma^+ \to p\pi^0$ with $\pi^0 \to \gamma\gamma$. The final state consists of a proton and a muon, giving two tracks in the spectrometer, two photons producing clusters in the LKr calorimeter and one unobserved anti-neutrino. The decay $\Xi^0 \to \Sigma^+\ell^-\overline{\nu}_\ell$ is the only source of Σ^+ particles in the neutral beam since the two-body decay $\Xi^0 \to \Sigma^+\pi^-$ is kinematically forbidden. Thus, the signal events were identified by requiring an invariant $p\pi^0$ mass consistent with the nominal Σ^+ mass value.

The Σ^+ decay was reconstructed using a positive charged track in the spectrometer (associated to the proton) and two clusters in the electromagnetic calorimeter (associated to the photons from $\pi^0 \to \gamma\gamma$ decay) within a time window of 2 ns. The longitudinal position of the Σ^+ decay vertex was determined using the π^0 mass constraint to calculate the distance of its decay point from the calorimeter:

$$\Delta z_{\pi^0} = \frac{1}{m_{\pi^0}}\sqrt{E_1 E_2 r_{12}^2} \tag{1}$$

where E_1 and E_2 are the measured energies of the two clusters and r_{12} is the distance between the two clusters in the transverse plane. Good candidates were kept if the reconstructed $p\pi^0$ invariant mass was within 6 MeV/c^2 of the nominal Σ^+ mass value. The mass interval was tightened from 8 MeV/c^2 to 6 MeV/c^2 with respect to the normalization channel (see below) to reduce the higher background contamination in the muon channel.

Muon identification was achieved by requiring the presence of in-time signals from the first two planes of the muon detector (±2 ns with respect to the time measured in the charged hodoscope). In addition, to reject pions and electrons, the energy deposited in the electromagnetic calorimeter in association to the muon track was required to be less than 2.5 GeV.

The lower momentum threshold for the muon track was set to 7 GeV/c (it was 4 GeV/c for the electron channel) to reduce the background contamination and to increase the efficiency for muon reconstruction (see section 7).

The muon momentum calculated in the Σ^+ rest frame was required to be less than 0.125 GeV/c, exploiting the fact that no contribution is expected from the signal sample above this limit. This cut was not applied in the normalization channel. Similarly, since the proton momentum in the signal sample is mostly above 54 GeV/c, this criterion was used to enhance the probability that sufficient energy is deposited in the electromagnetic and hadron calorimeters to satisfy the trigger condition $E_{\mathrm{HAC+LKr}} > 30$ GeV. In the normalization channel the lower cut on the proton momentum was set at 40 GeV/c.

The Ξ^0 decay vertex position was obtained by computing the closest distance of approach between the extrapolated Σ^+ line-of-flight and the muon track. This distance was required to be less than 4 cm. Furthermore, the deviation of the transverse Ξ^0 vertex position from the nominal line-of-flight defined by a straight line going from the center of the K_S target to the center of the liquid krypton calorimeter was required to be less than 3 cm.

The longitudinal position of the Ξ^0 vertex was required to be at least 6.5 m downstream of the K_S target, i.e. 0.5 m after the end of the final collimator and at most 40 m from the target. Similarly, the Σ^+ vertex position was required to be at least 6.5 m downstream of the target but at most 50 m from the target. The latter value was chosen larger than the upper limit for the Ξ^0 vertex position to account for the lifetime of the Σ^+ particle. The longitudinal separation between the Ξ^0 and Σ^+ decay vertices was required to be between -8 m and 40 m. The negative lower limit, tuned with Monte Carlo events, was chosen such as to take properly into account resolution effects.

The quantity $\vec{r}_{\mathrm{COG}}$ was defined as $\vec{r}_{\mathrm{COG}} = \sum_i \vec{r}_i E_i / \sum_i E_i$ where E_i is the energy of the detected particle and $\vec{r}_i$ the corresponding transverse position vector at the liquid krypton calorimeter position z_{LKr}. For a charged particle, the quantity $\vec{r}_i$ was obtained from the extrapolation to z_{LKr} of the upstream segment of the associated track. For kinematical reasons, the missing transverse momentum (p_t) is smaller in the muon case with respect to the electron case. Therefore $\vec{r}_{\mathrm{COG}}$ was required to be less than 8 cm instead of 15 cm as for the electron channel.

By requiring the invariant mass $\pi^+\pi^0\mu^-$ to be less than 0.490 GeV$/c^2$, the contamination from $K_L \to \pi^+\pi^-\pi^0$, when the π^- is misidentified as a muon, was reduced to a negligible level. This cut was not applied in the normalization channel.

Cuts were also applied on the positions of the hit points of the tracks in the chambers and on the cluster positions in the electromagnetic calorimeter to improve the trigger and the reconstruction efficiencies. Furthermore the energies of the photons coming from the π^0 decay were requested to be between 3 and 100 GeV to ensure linearity on the LKr measurement.

With the above selection criteria, 97 $\Xi^0 \to \Sigma^+\mu^-\overline{\nu}_\mu$ candidates were observed in the signal region. The distribution of events in the $p\pi^0$ invariant mass variable is shown in Figure 1 after all selection cuts were applied. Signal events peaking around the Σ^+ mass are clearly visible above the background.

A contribution to the background (about 20% of the total) comes from overlapping events in the detector (accidentals). This contribution was estimated directly from data samples, looking to the activity in the detectors not in time with the main event time. There is a small contribution to the background from the decay $\Xi^0 \to \Lambda\pi^0$ (populating the left side of the $p-\pi^0$ invariant mass distribution) with $\Lambda \to p\pi^-$ and with π^- either misidentified as a muon or decaying into $\pi^- \to \mu^-\nu_\mu$. This contribution was estimated by the Monte Carlo simulation. However the main contribution to the background is due to scattered events in the final collimator of the neutral beam, in analogy to what was seen in the normalization channel.

Due to the difficulty to simulate this contribution and due to the low statistics in the control samples coming from data, the background distribution in the $p\pi^0$ invariant mass was fitted with an exponential in the intervals 1.164-1.240 GeV$/c^2$ and 1.198 and 1.240 GeV$/c^2$. The fit was giving an estimate of $(30.8 \pm 3.8_{\mathrm{stat}} \pm 1.9_{\mathrm{syst}})$ background events when extrapolated into the signal region. The systematic uncertainty on the background level was estimated by varying the fitting function and the fit region (also including the signal region, with the signal fitted with a Gaussian distribution).

The data sample for the normalization channel $\Xi^0 \to \Sigma^+ e^-\overline{\nu}_e$ consists of 6316 events with a background of $(3.4 \pm 0.7)\%$.

A detailed description of the reconstruction and selection for the normalization channel is reported in [7]. For that decay, since the electron is completely absorbed in the LKr, the corresponding track was identified by requiring a ratio between the energy deposit in the LKr and the momentum measured by the spectrometer (E/p) greater than 0.85 and lower than 1.15. The other differences in the selection criteria of the signal and normalization channels are described above.

6 Acceptance

The acceptance for both signal and normalization decay channels was computed using a detailed Monte Carlo program based on GEANT3 [9, 10]. Particle interactions in the detector material as well as the response functions of the different detector elements were taken into account in the simulation. A detailed description of the generator of the electron channel can be found in [7]. The generator for the muon

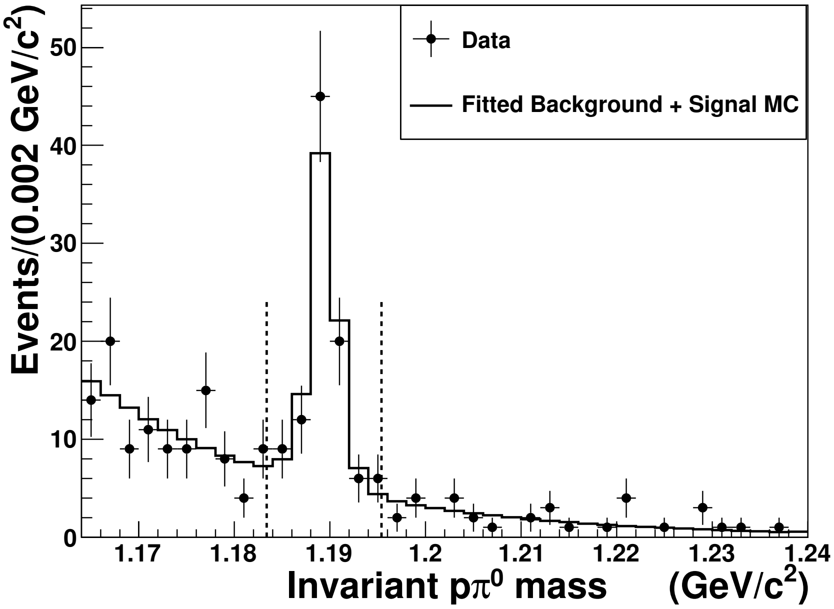

Fig. 1: Reconstructed pπ^0 invariant mass distribution for $\Xi^0 \to \Sigma^+ \mu^- \overline{\nu}_\mu$ candidates after all selection criteria were applied. Points with error bars are data. The peak at the Σ^+ mass value shows clear evidence for the signal. The vertical dashed lines delimit the signal region. The background was evaluated with a likelihood fit of the data performed in two intervals, between 1.164 and 1.180 GeV$/c^2$ and between 1.198 and 1.240 GeV$/c^2$. The solid histogram shows the sum of the background contribution (evaluated from the fit) and the Monte Carlo sample of the signal normalized to the events found in the data after background subtraction.

channel was modified to include the contribution from pseudo-scalar currents [11], parameterized with the form factor g_3 which, under Partially Conserved Axial Current (PCAC) hypothesis, can be extracted at $q = 0$ from the Goldberg-Treiman relation [12, 13]:

$$g_3(0)/f_1(0) = 2(M_{\Xi^0}/M_{K^-})^2 g_1(0)/f_1(0). \tag{2}$$

Since the g_3 term is multiplied by $m_{\text{lepton}}/m_{\Xi^0}$, its contribution is non-negligible for the muon case [11]. Using the available experimental results [7, 14, 15] for the electron channel, the best estimates for the remaining non-vanishing form factors are:

$$\begin{aligned} f_2(q^2=0)/f_1(q^2=0) &= 2.0 \pm 1.3 \\ g_1(q^2=0)/f_1(q^2=0) &= 1.21 \pm 0.05. \end{aligned} \tag{3}$$

The central values were plugged into the Monte Carlo generator and the corresponding errors where used to evaluate the systematic error related to the acceptance calculation. Radiative corrections were not included in the generator of the muon channel. This leads to a systematic uncertainty of 1%, estimated using the Monte Carlo simulation for the electron channel with the electron mass substituted by the muon one. The acceptance for the signal $\Xi^0 \to \Sigma^+ \mu^- \overline{\nu}_\mu$ was calculated to be (3.17 ± 0.01)%, while the acceptance for the normalization $\Xi^0 \to \Sigma^+ e^- \overline{\nu}_e$ was (2.49 ± 0.01)%. Both quoted uncertainties originate from the statistics of the Monte Carlo samples.

7 $\Xi^0 \to \Sigma^+ \mu^- \overline{\nu}_\mu$ branching ratio

The $\Xi^0 \to \Sigma^+ \mu^- \overline{\nu}_\mu$ branching ratio was obtained from the background-subtracted numbers of selected events for signal and normalization, the corresponding acceptance values, the normalization branching ratio [7] and the efficiency on muon identification. These quantities are summarized in Table 1 and yield:

$$\text{BR}(\Xi^0 \to \Sigma^+ \mu^- \overline{\nu}_\mu) = (2.17 \pm 0.32_{\text{stat}} \pm 0.17_{\text{syst}}) \times 10^{-6}, \tag{4}$$

where the statistical uncertainty originates from the event statistics and the systematic one is the sum in quadrature of the various contributions presented in Table 2.

Table 1: Parameters used for the BR($\Xi^0 \to \Sigma^+ \mu^- \overline{\nu}_\mu$) measurement.

	$\Xi^0 \to \Sigma^+ \mu^- \overline{\nu}_\mu$	$\Xi^0 \to \Sigma^+ e^- \overline{\nu}_e$
Event statistics	97	6316
Background	(30.8 ± 4.2) events	$(3.4 \pm 0.7)\%$
Acceptance	$(3.17 \pm 0.01)\%$	$(2.49 \pm 0.01)\%$
Muon inefficiency	$(1.5 \pm 0.5)\%$	
Branching ratio		$(2.51 \pm 0.03_{\text{stat}} \pm 0.09_{\text{syst}}) \times 10^{-4}$

The largest contribution to the total systematic uncertainty comes from the background subtraction, described above.

From the systematic uncertainty related to the measurement of the branching ratio of the normalization channel, the trigger efficiency contribution was eliminated, since it is common to both channels. A further systematic of 3% was added to take into account the dependence of the trigger efficiency on the lepton momentum.

The sensitivity of the branching ratio measurement to the form factors was studied by varying $g_1(0)/f_1(0)$ and $f_2(0)/f_1(0)$ within the limits provided by their uncertainties and doubling or neglecting the $g_3(0)$ value. The muon momentum distribution from Monte Carlo simulation was divided by the distribution of muon efficiency as a function of muon momentum as measured from $K^\pm \to \mu^\pm \nu_\mu$ $(K\mu 2)$ decays,

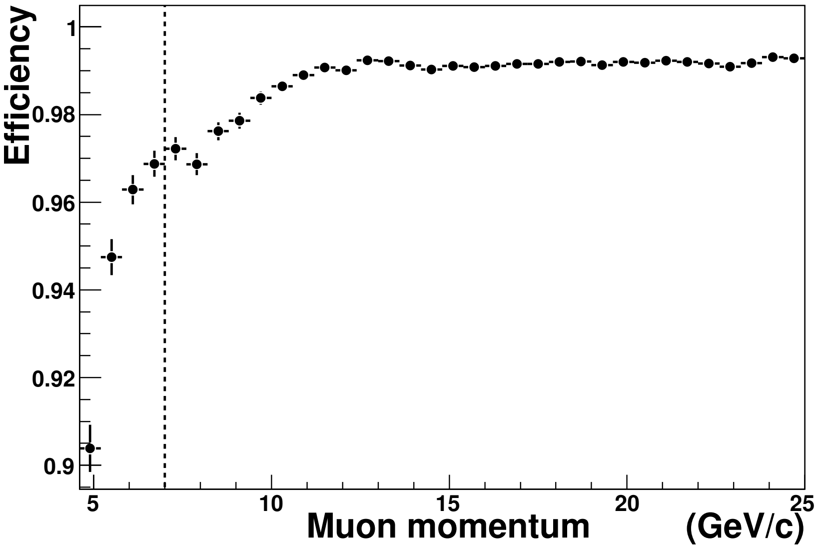

Fig. 2: Efficiency for muon identification as a function of muon momentum (right), the dashed line shows the lower threshold at 7 GeV/*c* applied to muon momentum.

obtained from a large sample collected in 2003 (see Figure 2). A consistent result was obtained by considering $K^0 \to \pi^\pm \mu^\mp \nu$ decays collected in 2002 but with much lower statistics. The resulting correction of $(+1.5 \pm 0.5)\%$ was applied in the BR calculation.

Table 2: Sources of systematic uncertainties.

Source	Uncertainty
Background	±6.4%
Normalization	±3.0%
L2 trigger efficiency	±3.0%
Form factors	±1.5%
Radiative corrections	±1.0%
Muon reconstruction efficiency	±0.5%
Total	±7.9%

8 Conclusion

Using data collected in 2002 with the NA48 detector at CERN, we obtaine the first clear evidence of the decay $\Xi^0 \to \Sigma^+ \mu^- \overline{\nu}_\mu$, with a precision on the branching ratio being significantly better than the existing published value. This result is in good agreement with the branching ratio measured by the NA48/1 collaboration for the electron channel, once the theoretical ratio of the corresponding decay amplitudes is taken into account[3].

Acknowledgments

It is a pleasure to thank the technical staff of the participating laboratories, universities and affiliated computing centres for their efforts in the construction of the NA48 apparatus, in the operation of the experiment, and in the processing of the data.

References

[1] N. Cabibbo, Physical Review Letters 10 (1963) 531.

[2] J.F. Donoghue,B.R. Holstein and S.W. Klimt, Phys. Rev. D 35 (1987) 934.

[3] R. Flores-Mendieta, A. Garcia and G. Sanchez-Colon, Phys.Rev. D54 (1996) 6855.

[4] F. Schlumpf, Phys. Rev. D 51 (1995) 2262.

[5] A. Krause, Helv. Phys. Acta 63 (1990) 3.

[6] J. Anderson and M.A. Luty, Phys. Rev. D 47 (1993) 4975.

[7] J.R. Batley et al. (NA48/1 Collaboration), Physics Letters B 645 (2007) 36.

[8] A. Alavi-Harati et al. (KTeV Collaboration), Physical Review Letters 95 (2005) 081801.

[9] V. Fanti et al. (NA48 Collaboration), Nuclear. Instrum. Meth. A 574 (2007) 433.

[10] GEANT Description and Simulation Tool, CERN Program Library Long Writeup W5013 (1994) 1.

[11] A. Kadeer, J. G. Korner and U. Moosbrugger Eur. Phys. J. C 59 (2009) 27.

[12] M. L. Goldberger, S. B. Treiman, Physical Review 111 (1958) 354.

[13] E. D. Commins, P. H. Bucksbaum, “Weak interactions of leptons and quarks”, Cambridge University Press (2001).

[14] A. Alavi-Harati et al. (KTeV Collaboration), Physical Review Letters 87 (2001) 132001.

[15] J. Beringer et al. (Particle Data Group), Phys. Rev. D 86 (2012) 010001.